# Delamination Modelling Using an Element Free Galerkin Approach

E. Barbieri, M. Meo [1]
Material Research Centre
Department of Mechanical Engineering
University of Bath, BA2 7AY Bath UK

**Abstract**
The prediction of delamination initiation and propagation in composite structures is quite complex, and requires advanced modelling techniques. The main computational techniques currently used include for example the finite element method, the boundary integral method and others. While current computational tools are quite robust for the modelling of stationary cracks, the representation of crack evolution of arbitrary cracks is still yet to be addressed properly due to the difficulties in relating an evolving geometry to the discretization for each stage of the delamination propagation. The objective of the paper is to investigate the potential of the Element-Free Galerkin (EFG) method coupled to a material cohesive zone damage model for simulating the steady-state evolution of delamination in composite structures for quasi-static loading mode I. In particular, a single relative displacement-based damage parameter is applied in a softening law to track the damage state of the layers interface and to prevent the restoration of the undamaged cohesive state during unloading. The methodology developed was used to simulate delamination growth in a 24-ply unidirectional AS4/PEEK (APC2) carbon fibre reinforced composite for a single mode delamination test specimen, i.e. the Double Cantilever Beam (DCB). To demonstrate the accuracy of the proposed methodology, the results were compared with experimental data showing promising accuracy and robustness.

***Keywords*** Delamination, cohesive zone damage model, Element-Free Galerkin

## 1. Introduction

Delamination is one of the prevalent forms of failure in laminated composites due to the absence of reinforcement in the thickness direction. As a result of impact or a manufacturing defect, delaminations can cause a significant drop in the compressive load carrying capacity. In order to improve and predict the behaviour of composite materials under static and dynamic loading, analysis tools capable of modelling progressive failure for various damage modes are needed. The objective of this work is to present modelling techniques to simulate progressive debonding or delamination with an Element Free Galerkin (EFG) method. Our attention was focused on the simulation of delamination growth in a double cantilever beam test, which is seen as a mode I fracture.

## 2. The Element Free Galerkin Method

A *meshless* discretization consists in only nodes and approximating functions do not rely on a mesh-based construction or an element-based construction such as in the Finite Element (FE) (Shaofan and Kam, 2002), (Liu,2003). Thus, conversely to FE when shape functions and integrals are evaluated element-wise and then assembled, in meshfree (or meshless) methods (MM) shape functions are defined on the whole domain $\Omega$ and integrals for the construction of the matrices are usually evaluated numerically with a subdivision of the entire domain in quadrature cells (Dolbow and Belytschko, 1998) and (Dolbow and Belytschko, 1999).
The practical use of MM over FE is due to fact that remeshing is avoided and this is particularly useful in a whole range of problems including large deformations, moving

[1]Corresponding Author: m.meo@bath.ac.uk Tel +441225384224 Fax: +441225386928

discontinuities (such as cracks) and fracture mechanics as explained in (Fries and Matthies, 2003).. The most common approximating functions in MM methods are *moving least squares (MLS) functions*, obtained through a weighted least squares procedure where the weights are spatial functions that span all over the domain Ω.
More detailed information about their mathematical properties and expressions of shape functions can be found in (Belytschko et al., 1996b).
Using *MLS* it can be shown that

$$u^h(x) = \sum_{I=1}^{N} \phi_I(x) U_I \tag{1}$$

where $u^h(x)$ is the MLS approximation of the function *u(x),* $\phi_I(x)$ is the *i-th* shape function figure 1, *N* is the number of nodes and $U_I$ are the nodal values. Shape functions are obtained resolving a linear system of equations for each point of evaluation

$$\phi_I(x) = p(x)^T A^{-1}(x) B(x) \tag{2}$$

Where *A* is called the moment matrix

$$A(x) = \sum_{I=1}^{N} w(x - x_I)\, p(x_I)\, p(x_I)^T \tag{3}$$

$$B(x) = [w(x - x_1)\, p(x_1)^T \quad w(x - x_2)\, p(x_2)^T \quad \ldots \quad w(x - x_N)\, p(x_N)^T] \tag{4}$$

Where $w(x-x_i)p(x_i)^T$ is a weighting function which extents around a disk centered in each node. The radius of this disk is called dilatation parameter and p(x) are called basis functions for example

$$p(x)^T = [1 \quad x \quad x^2 \quad \ldots \quad x^k] \tag{5}$$

in 1D case or

$$p(x)^T = [1 \quad x \quad x^2 \quad xy \quad y \quad y^2] \tag{6}$$

in 2D case. It should be clear that MLS is a least squares method, thus it does not interpolate prescribed values $U_I$ at the nodes $x_I$

$$u^h(x_J) \neq U_I \tag{7}$$

for this reason, MLS is an approximation method rather than an interpolation method. Because of equation (7), MLS shape functions do not satisfy the Kronecker condition, as it can also seen from figure 1

$$\phi_I(x_J) \neq \delta_{IJ} \tag{8}$$

The EFG method (Dolbow and Belytschko, 1998),(Belytschko et al., 1996b) is based on the weak variational form of the differential equations of the elasticity along with the boundary conditions

$$\int_\Omega \delta\varepsilon^T \sigma d\Omega - \int_\Omega \delta u^T b d\Omega - \int_\Gamma \delta u^T t d\Gamma + \int_\Omega \delta u^T \rho \ddot{u} d\Omega + \alpha \int_{\Gamma_u} \delta G(u)^T G(u) d\Gamma_u = 0 \tag{9}$$

where Ω is the entire domain of the solid, *Γ* its whole boundary, $\Gamma_u$ the part of boundary where are imposed the *essential boundary conditions*, $\boldsymbol{\sigma}$ is the vectorized stress tensor, $\boldsymbol{\varepsilon}$ is the

vectorized strain tensor, $\rho$ the mass density, $\boldsymbol{u}$ is the displacements vector, $\boldsymbol{b}$ and $\boldsymbol{t}$ are respectively the body and the surface forces and $\boldsymbol{G(u)}$ the vector of the essential boundary conditions, for example in *2D*

$$G(u) = \begin{bmatrix} u(x) - \bar{u}(x) \\ v(x) - \bar{v}(x) \end{bmatrix} \forall x \in \Gamma_u \tag{10}$$

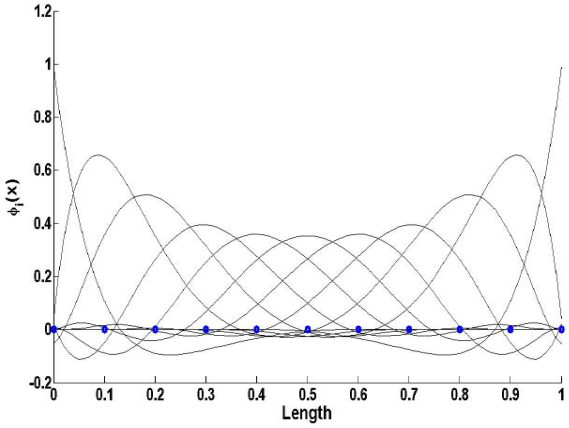


**Figure 1: MLS Shape Functions: dotted line: nodes, continuos line: shape functions**

The parameter α is a *penalty parameter* used to impose essential boundary conditions. In fact, as in eq. (1), because of the non-interpolating nature of MLS, essential boundary conditions cannot directly being imposed on the nodes. Thus, a penalty method is needed for enforcing boundary conditions on displacements. Substitution of eq. (1) in eq. (9) leads to the discretized equation of motion

$$M\ddot{U} + C\dot{U} + KU = F(t) \tag{11}$$

where $\boldsymbol{M}$ is the mass matrix, $\boldsymbol{C}$ is the damping matrix, $\boldsymbol{K}$ is the stiffness matrix and $\boldsymbol{F}$ is the vector of generalized forces. It should be remarked that $\boldsymbol{U}$ is a "fictitious" nodal displacements vector because of eq. (7). Mass and stiffness matrices are given by

$$M_{IJ} = \int_{\Omega} \rho \phi_I \phi_J d\Omega \tag{12}$$

$$K_{IJ} = \int_{\Omega} L_I^T D L_j d\Omega + \alpha \int_{\Gamma_u} \phi_I \phi_J d\Gamma_u \tag{13}$$

where $\boldsymbol{L}$ the linear differential operator of the strain applied to all shape functions, D is the linear stress-strain relationship matrix.

$$f(t) = \int_{\Omega} \phi^T b d\Omega + \int_{\Gamma} \phi^T t d\Gamma + \int_{\Gamma_u} \phi^T \bar{u} d\Gamma_u \tag{14}$$

## 3. The Cohesive Zone Model

Placing interfacial decohesion elements between composite layers is the most common technique to simulate delamination growth with FE. Nevertheless, since no elements are used in meshfree methods, decohesion region has to be implemented, which means that softening is applied to those points within the resin thickness. A decohesion failure criterion that considers

both the aspects of a strength-based analysis and fracture mechanics was used to simulate debonding by softening the region among the laminate. The interface is characterized by constitutive equations which take into account the applied stress $\boldsymbol{\sigma}$ to the relative displacement $\boldsymbol{\delta}$ at the interface. The stress – relative displacement curve is divided into three main parts (fig. 2) and the constitutive equations are the following:

- $\delta \le \delta_0$ : *elastic part*: traction across the interface increases until it reaches a maximum, and the stress is linked to the relative displacement via the interface stiffness $\sigma = k_{1b}\delta$
- $\delta_0 < \delta \le \delta_F$ : *softening part*: the traction across the interface decreases until it becomes equal to zero: the two layers begin to separate. The damage accumulated at the interface is represented by a variable *d*, which is equal to zero when there is no damage and reaches 1 when the material is fully damaged;
- $\delta \le \delta_F$ : *decohesion part*: decohesion of the two layers is complete: there is no more bond between the two layers, the traction across the interface is null

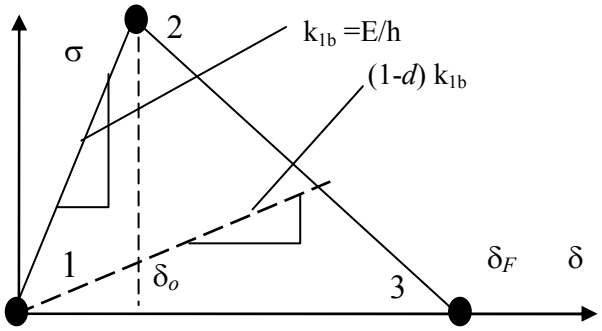


**Figure 2. Bilinear softening model**

The area under the curve is the fracture energy $G_{IC}$ for this particular mode. The delamination implemented consists in a criterion based on the stress and the relative displacements of the two layers above and underneath the resin zone. If they satisfy the condition of the bilinear model, then their elastic properties are changed. The global stiffness matrix is hence calculated using the constitutive equations of the softening bilinear model. The specimen was clamped at one end, and displacements were applied on the upper and lower faces of the plate. A cubic load distribution (figure 3) is used in order to get the displacements field of a cantilevered beam when a concentrated force is applied on the other end. In order to define the constitutive equation for the resin, the penalty parameter and the interlaminar tensile strength had to be determined. The properties necessary to define a bilinear interfacial softening behaviour are the interlaminar tensile strength and the fracture energies. Careful must be taken in the choice of the penalty stiffness, since too low of a value brings to an inaccurate representation of the bonding behaviour of the resin. Conversely, a big penalty parameter could lead to numerical instabilities. Another important parameter of the analysis is the increment of applied displacement at each load step. In this case, a small increment brings to more accurate results but with the drawback of a longer computation time. A bigger increment instead brings to an immediate delamination without softening causes a rapid decrease in the interlaminar stress and thus of the reaction force. Different cases with different penalty stiffness were considered.

## 4. Double Cantilever Beam Results

The problem analysed was a double cantilever beam (DCB) test used to determine mode I

toughness. The DCB test specimen was made of a unidirectional fiber-reinforced laminate. The specimen was 0.185-m long, 0.025 m wide, with two 2.5-mm thick plies. The DCB test specimen was made $(0)_{24}$ from a carbon fiber-reinforced polyetheretherketone (C/PEEK) laminate (APC-2/AS4). The laminate material properties are reported in Table 1.

| $E_{11}$ | $E_{22}=E_{33}$ | $G_{12}=G_{13}$ | $G_{23}$ | $\nu_{12}$ | $\nu_{13}$ | $\nu_{23}$ |
|---|---|---|---|---|---|---|
| 135 Gpa | 9 Gpa | 5.2 Gpa | 1.9 GPa | 0.34 | 0.34 | 0.46 |

**Table 1. Properties for APC-2/AS4-CFRP**

Analyses were also conducted for different penalty stiffness and different nodes distribution. Regular arrangements of nodes along both axes were used. Four different distributions include 5x30 nodes, 15x30 nodes, 20x30 nodes and 30x30 nodes. The model implemented is a plane strain model. Gaussian quadrature of degree *2*, using the same number of cells as that of nodes, was used for the evaluation of the integrals. Penalty stiffnesses are automatically defined with the choice of $\delta_0$. The smaller this value, the higher is the penalty stiffness.

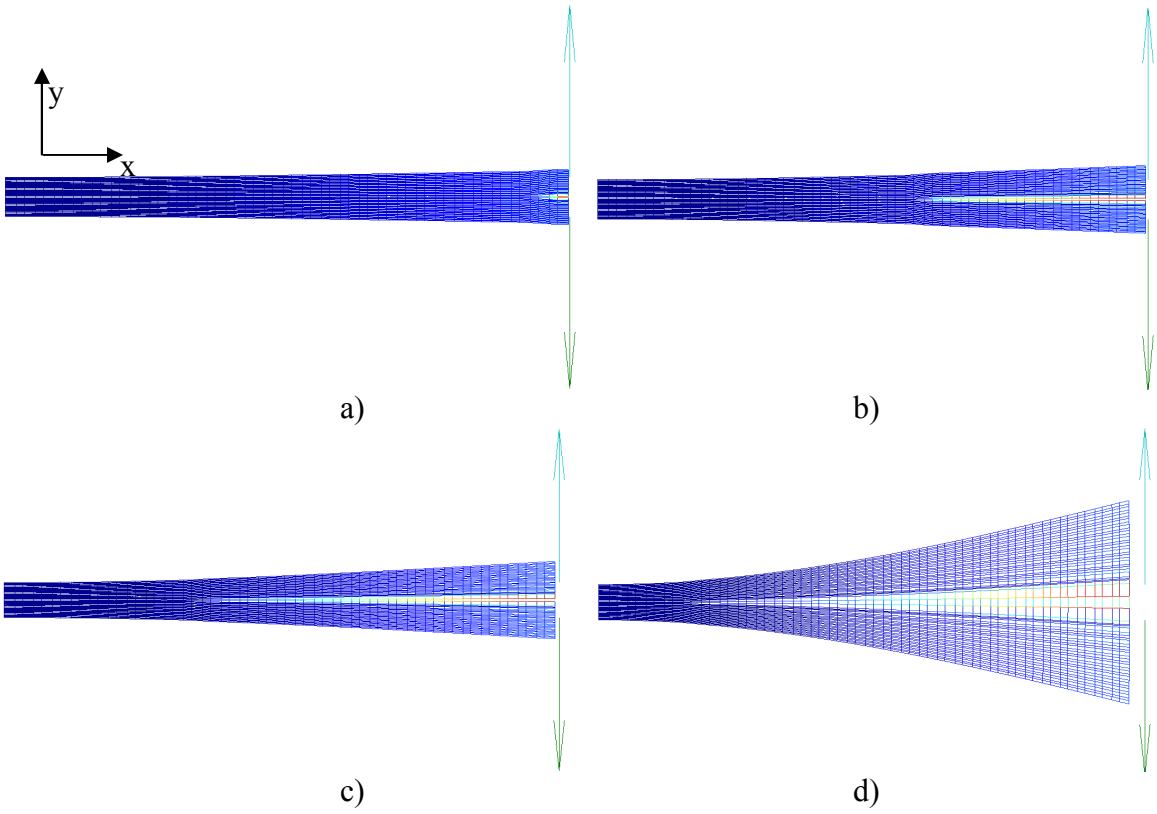


**Figure 3. Propagation of Delamination for different stages: a) Start b) initial propagation c) Middle stage Propagation d) Complete; Colormap shows damage variable d: blue:d=0, red: d=1;**

Figures 3 illustrate four different stages of delamination, including initiation and complete delamination. Colours indicate the intensity of damage *d* used to soften the elastic properties as explained in section 3. It can be clearly seen how the delamination propagates through the half-plane of the plate, reaching the constrained edge on the left. The reaction force ***F*** has been calculated according to the definition of interlaminar stress, using the penalty stiffness and the relative displacement (Pantano and Averill, 2004)

$$F = \int_A k_{1b}(\delta v)\delta v dx dz \tag{15}$$

where A is the part of interface along x and z (along the width of the plate) still in contact

during the delamination. This force is plotted against the displacement at the end point of the upper face of the plate.

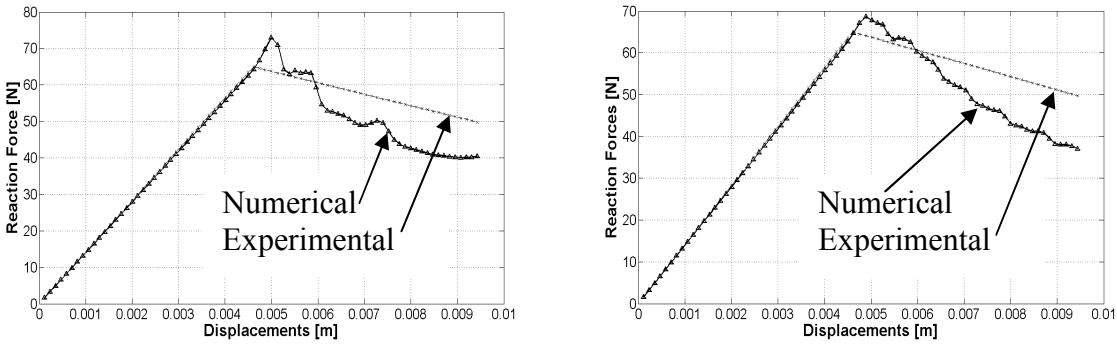


**Figure 4. Force-displacement curve for different nodes distribution; a) coarse b) fine**

Node distribution sensitivity analysis was conducted. As it could be seen in fig 4.a, a low number of nodes in the x-direction 15 (y-direction 30), could lead instead to a wrong representation of the resin thickness and thus premature delamination, i.e. poor post damage behaviour. In figure 5b, it is shown that by increasing the number of nodes in the x-direction to 20 (y-direction 30) brings to a smoother graph after the initiation of delamination since there are more quadrature cells and thus the quadrature is more accurate.

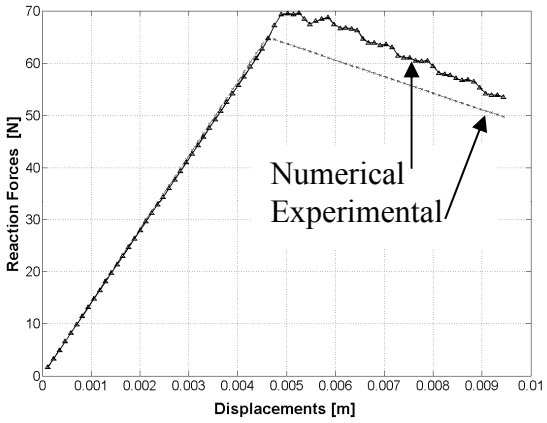


**Figure 5. Force-displacement curve –Final Model**

Sensitivity analysis of the nodes in the y-direction was performed. The results showed that a decrease of the nodes led to wrong representation of the resin thickness and thus premature delamination. These results, however, show that also for the EFG method, as for the finite element analysis, by increasing the number of nodes leads to more accurate representation of the delamination failure. Finally, figures 5 show the unloading response once delamination occurs compared to the experiments in (Camanho et al., 2001, 2002, 2003) for an optimised number of nodes (x-direction/y-direction 30x30). Such findings were similar also found with finite elements analysis. As it can be seen, the unloading is bilinear, as assumed in the decohesion model. Moreover there is good agreement with the experiments. In each case, the maximum estimated reaction force is around 70 N for a displacement of $\delta$=4.9e-3 m against an experimental value of 65 N for $\delta$ = 4.6e-3 m.

## 5. Conclusions

The objective of the present work was to present a new numerical technique able to predict delamination failure mode in composite structures. In particular, this paper investigated the potential of the Element-Free Galerkin (EFG) method coupled to a material cohesive zone damage model to simulate the steady-state evolution of crack growth under quasi-static loading. Delamination growth of a double cantilever beam test (DCB) was proposed. Results showed that for the particular studied delamination phenomena, the proposed modelling technique is capable of predicting the delamination growth in a double cantilever beam with acceptable results in the linear regime, while some discrepancies were found. Future work will involve further validation of these modelling techniques to model more complex structures and other delamination failure modes.

## References


1. T. Belytschko, Y. Krongauz, M. Fleming, D. Organ, and W. Snm Liu. Smoothing and accelerated computations in the element free Galerkin method. Journal of Computational and Applied Mathematics, 74(1):111–126, 1996a.
2. T. Belytschko, Y. Krongauz, D. Organ, M. Fleming, and P. Krysl. Meshless methods: an overview and recent developments. Computer Methods in Applied Mechanics and Engineering, 139(1):3–47, 1996b.
3. P. Camanho and C. Davila. Mixed-mode decohesion finite elements for the simulation of delamination in composite materials. NASA-Technical Paper, 211737, 2002.
4. P. Camanho, C. Davila, and D. Ambur. Numerical Simulation of Delamination Growth in Composite Materials. NASA Langley Technical Report Server 2001
5. P. Camanho, C. Davila, and M. de Moura. Numerical Simulation of Mixed-Mode Progressive Delamination in Composite Materials. Journal of Composite Materials, 37(16):1415, 2003.
6. J. Chen, M. Crisfield, A. Kinloch, E. Busso, F. Matthews, and Y. Qiu. Predicting Progressive Delamination of Composite Material Specimens via Interface Elements. Mechanics of Advanced Materials and Structures, 6(4): 301–317, 1999.
7. J. Dolbow and T. Belytschko. An introduction to programming the meshless element free Galerkin method. Archives of Computational Methods in Engineering, 5(3):207–241, 1998.
8. J. Dolbow and T. Belytschko. Numerical integration of the Galerkin weak form in meshfree methods. Computational Mechanics, 23(3):219–230, 1999.
9. T. Fries and H. Matthies. Classification and overview of meshfree methods. Brunswick, Institute of Scientific Computing, Technical University Braunschweig, Germany. Informatikbericht Nr, 3, 2003.
10. G. Liu. Mesh Free Methods: moving beyond the finite element method. CRC Press, 2003.
11. M. Meo and E. Thieulot. Delamination modelling in a double cantilever beam. Composite Structures, 71(3-4): 429–434, 2005.
12. Pantano and R. Averill. A mesh-independent interface technology for simulation of mixed-mode delamination growth. International Journal of Solids and Structures, 41(14):3809–3831, 2004.
13. L. Shaofan and L. Kam. Meshfree amd Particle Methods and Their Applications. Applied Mechanics Review, 55:1–34, 2002.
14. C. Sun and S. Zheng. Delamination characteristics of double-cantilever beam and end-notched flexure composite specimens. Composites Science and Technology, 56(4):451–459, 1996.